



Published in final edited form as:

Nat Chem. 2014 July ; 6(7): 635–643. doi:10.1038/nchem.1963.

Development of a minimal saponin vaccine adjuvant based on QS-21

Alberto Fernández-Tejada¹, Eric K. Chea², Constantine George³, NagaVaraKishore Pillarsetty⁴, Jeffrey R. Gardner¹, Philip O. Livingston^{3,⊥}, Govind Ragupathi³, Jason S. Lewis⁴, Derek S. Tan^{1,2,5,*}, and David Y. Gin^{1,2,5,‡}

Govind Ragupathi: ragupatg@mskcc.org; Jason S. Lewis: lewisj2@mskcc.org; Derek S. Tan: tand@mskcc.org

¹Molecular Pharmacology & Chemistry Program, Memorial Sloan-Kettering Cancer Center, 1275 York Avenue, New York, New York 10065

²Pharmacology Program, Weill Cornell Graduate School of Medical Sciences, Memorial Sloan-Kettering Cancer Center, 1275 York Avenue, New York, New York 10065

³Melanoma & Immunotherapeutics Service, Department of Medicine, Memorial Sloan-Kettering Cancer Center, 1275 York Avenue, New York, New York 10065

⁴Radiochemistry & Imaging Science Service, Department of Radiology, Memorial Sloan-Kettering Cancer Center, 1275 York Avenue, New York, New York 10065

⁵Tri-Institutional Research Program, Memorial Sloan Kettering Cancer Center, 1275 York Avenue, New York 10065, USA

Abstract

Adjuvants are materials added to vaccines to enhance the immunological response to an antigen. QS-21 is a natural product adjuvant under investigation in numerous vaccine clinical trials, but its use is constrained by scarcity, toxicity, instability, and an enigmatic molecular mechanism of action. Herein, we describe the development of a minimal QS-21 analogue that decouples adjuvant activity from toxicity and provides a powerful platform for mechanistic investigations. We found that the entire branched trisaccharide domain of QS-21 is dispensable for adjuvant activity and that the C4-aldehyde substituent, previously proposed to bind covalently to an unknown cellular target, is also not required. Biodistribution studies revealed that active adjuvants were retained at the injection site and nearest draining lymph nodes preferentially compared to attenuated variants. Overall, these studies have yielded critical insights into saponin structure–function relationships,

Users may view, print, copy, and download text and data-mine the content in such documents, for the purposes of academic research, subject always to the full Conditions of use:http://www.nature.com/authors/editorial_policies/license.html#terms

Address correspondence and requests for material to D.S.T.

[⊥]Present Address: Adjuvance Technologies Inc., 116 W 22nd St., Suite #1, New York, NY 10011

[‡]Deceased March 22, 2011.

Author Contributions: A.F.-T., E.K.C., N.P., J.R.G., G.R., J.S.L., D.S.T., and D.Y.G. conceived and designed the experiments. A.F.-T. and E.K.C. performed the syntheses. C.G. performed the preclinical mouse vaccination experiments. C.G. and N.P. performed the biodistribution experiments. J.R.G. performed the fluorescence imaging experiments. A.F.-T., E.K.C., N.P., J.R.G., P.O.L., G.R., J.S.L., D.S.T., and D.Y.G. analyzed the data. A.F.-T. and D.S.T. wrote the manuscript.

Author Conflicts: J.R.G., P.O.L., G.R., and D.Y.G. are founders of Adjuvance Technologies Inc., and have financial interests in the company.

provided practical synthetic access to non-toxic adjuvants, and established a platform for detailed mechanistic studies.

Molecular vaccines comprised of subunit antigens are often less immunogenic than whole pathogens and do not elicit adequate immune responses alone, requiring the inclusion of an immunoadjuvant to increase immunogenicity^{1,2}. Unfortunately, few adjuvants are sufficiently potent and non-toxic for clinical use³. QS-21, a saponin natural product from the *Quillaja saponaria* tree⁴, is one of the most promising adjuvants currently under investigation (Figure 1a)⁵. It is composed of two isomeric constituents, QS-21-apiose (**1a**) and QS-21-xylose (**1b**)⁶, which differ at the terminal sugar in the linear tetrasaccharide domain⁷. QS-21 has emerged as the immunopotentiator of choice in many recent clinical trials and vaccines containing QS-21 are under development for several cancers⁸ and infectious and neurodegenerative diseases (malaria⁹, HIV¹⁰, hepatitis¹¹, tuberculosis¹², Alzheimer's disease¹³). Despite its promise, QS-21 suffers from several liabilities including limited access from its natural source, toxic side effects, and chemical instability due to spontaneous hydrolysis of the acyl chain. Furthermore, poor understanding of its molecular mechanism of action impedes rational development of analogues with improved efficacy and decreased toxicity.

To address these challenges, our group previously achieved the first chemical synthesis of QS-21¹⁴⁻¹⁵. Subsequent studies revealed that simplified acyl chain domain variants having stable amide linkages retain adjuvant activity and exhibit decreased toxicity¹⁶. More recently, systematic truncation of the linear tetrasaccharide domain identified a trisaccharide variant with improved synthetic accessibility, albeit with reemergence of toxicity¹⁷. Amine **2** (SQS-0-0-5-11) was also identified as an adjuvant-inactive precursor that could be converted to active adjuvant **3** (SQS-0-0-5-12), the first fluorescent saponin with potent adjuvant activity (Figure 1b). In subcellular localization studies, **3** was internalized into dendritic cells, while two other fluorescent saponins with weak adjuvant activity were not¹⁷.

Herein, we report systematic structure–function studies of the two remaining structural domains of QS-21 that have led to the development of a minimal saponin adjuvant that is both synthetically accessible and successfully decouples adjuvant activity from toxicity. Most strikingly, the entire branched trisaccharide domain proved dispensable for adjuvant activity in these synthetic saponins. This enabled targeted modifications in the triterpene domain that revealed that the C4-aldehyde substituent, previously suggested to be involved in covalent binding to a putative cellular target of QS-21¹⁸, is not required for adjuvant activity. Moreover, incorporation of an aryl iodide motif in the acyl chain domain enabled biodistribution studies of active/attenuated pairs of radioiodinated saponins in mice, demonstrating preferential accumulation of active adjuvants at the site of injection and within the nearest draining lymph nodes. Complementary studies with fluorescent probes show that co-administration with an active adjuvant increases localization of the antigen ovalbumin (OVA) to the lymph nodes, suggesting a potential role for antigen trafficking in the mechanism of action of these saponin adjuvants.

Results

Initial Evaluation of Iodinated Saponins **6** and **8**

In our initial efforts, we sought to introduce a radioiodine (^{131}I) into the QS-21 saponin scaffold to enable *in vivo* biodistribution studies. We first synthesized the non-radiolabeled aryl iodide **6** (SQS-0-0-5-18) by acylation of amine **2** (SQS-0-0-5-11)¹⁷ (Figure 1b). Because no *in vitro* model exists to assess adjuvant activity, biological evaluation of aryl iodide **6** was carried out in a preclinical mouse vaccination model involving a multi-antigen formulation comprised of the immunogenic peptide MUC1 (mucin-1, prostate and breast cancer antigen, non-glycosylated tandem repeat domain) conjugated to the highly immunogenic KLH carrier protein (MUC1-KLH) and OVA, a reliable immunogen that induces both antibody and T-cell responses in mice. Antibody responses against each of the three antigens, co-administered with the adjuvant of interest, were determined by ELISA (see Supplementary Methods).

Aryl iodide saponin **6** (SQS-0-0-5-18) induced antibody titers comparable to both NQS-21 (natural QS-21) and SQS-21 (synthetic QS-21, 65% **1a** and 35% **1b**) (Figure 1d–f) and also exhibited reduced toxicity compared to QS-21, as assessed by mouse weight loss (Figure 1g). As a negative control, we also synthesized the iodinated saponin variant **8** (SQS-0-3-7-18), which lacks the linear tetrasaccharide domain (Figure 1c and Supplementary Fig. 1) and exhibited poor adjuvant activity (Supplementary Fig. 1).

Biodistribution of Radioiodinated Saponins [^{131}I]-**6** and [^{131}I]-**8**

For biodistribution studies, we synthesized radiolabeled aryl iodide saponin [^{131}I]-**6** ([^{131}I]-SQS-0-0-5-18) via aryl tin–halide exchange¹⁹ of trimethylstannane **7** (Figure 1b). Radioiodinated [^{131}I]-**8** ([^{131}I]-SQS-0-3-7-18) was synthesized analogously from **9** as a negative control (Figure 1c).

To identify tissues and organs that could play roles in saponin mechanisms of action, we compared the acute *in vivo* biodistribution of the active adjuvant [^{131}I]-**6** and the attenuated adjuvant [^{131}I]-**8** in mice co-administered with OVA. Treatment with [^{131}I]-**6**, compared to [^{131}I]-**8**, resulted in significantly higher recovery of radioactivity at the site of injection (17-fold higher, 78% ID/g [injected dose per gram]) and in the nearest draining lymph nodes (24-fold higher, 27% ID/g) at 24 h post-injection (Figure 2a), which was retained at 72 h and 96 h post-injection (Supplementary Fig. 2). In contrast, radioactivity in other tissues where large fold-differences were initially observed (muscle, bone, skin) decreased rapidly at the later timepoints. Minimal deiodination of [^{131}I]-**6**, evidenced by low thyroid uptake (0.21% ID/g), was observed at 24 h (Figure 2a), although deiodination increased at later time-points (Supplementary Fig. 2). In contrast, the attenuated adjuvant [^{131}I]-**8** was recovered at significantly lower levels at the site of injection (4.5% ID/g) and nearest draining lymph nodes (1.1% ID/g) at 24 h post-injection (Figure 2a) and was further cleared from both sites at later time-points (Supplementary Fig. 2). Taken together, these data indicate that only the active adjuvant **6** (SQS-0-0-5-18) localizes to and is retained at the injection site and lymph nodes, while the attenuated adjuvant **8** (SQS-0-3-7-18) is not.

Other adjuvants that contain mixtures of *Quillaja* saponins have previously been reported to affect the biodistribution of antigens^{20,21}, although it is not known whether biodistribution of the adjuvant is influenced by the presence or absence of the antigen. To investigate these effects with these structurally-defined QS-21 variants, we assessed the biodistribution of active adjuvant [¹³¹I]-**6** and inactive adjuvant [¹³¹I]-**8** in absence of OVA (Supplementary Fig. 3). In both cases, the biodistribution profiles were comparable to those observed in the presence of OVA above (Supplementary Fig. 2), indicating that the antigen OVA does not impact the biodistribution of these saponin adjuvants.

In a complementary experiment, we examined the biodistribution of [¹³¹I]-OVA in the presence and absence of active adjuvant **6** (Supplementary Fig. 4). Although comparable biodistribution profiles resulted, thyroid uptake was also high, indicative of rapid deiodination of [¹³¹I]-OVA, which is commonly observed for radioiodinated proteins. Thus, the influence of **6** upon OVA antigen biodistribution could not be assessed effectively and an alternative experimental approach was required.

To address this problem, we conducted *in vivo* fluorescence imaging experiments with fluorescein-labeled active adjuvant **3** (SQS-0-0-5-12)¹⁷ and Alexa-647-conjugated OVA (OVA-A647). At 24-h post-injection, we observed retention of the fluorescent saponin at the injection site (Figure 2b) and accumulation within the draining lymph nodes (left node in Figure 2c), consistent with the biodistribution results above. Immunohistochemical analysis of dissected nodes indicated subnodal localization of **3** to the cortex of the draining inguinal node. Flow cytometric analysis demonstrated dendritic-cell-specific internalization of **3** within the lymph nodes.¹⁷ Moreover, while OVA-A647 was observed at the site of injection in mice treated with both the active adjuvant **3** and an unlabeled, inactive adjuvant **2** (SQS-0-0-5-11) (Figure 2b and Supplementary Fig. 5), it only localized to the nearest draining lymph nodes when co-injected with the active adjuvant **3** (Figure 2c). Overall, these data suggest a role for the active saponin **3** in the trafficking of the OVA antigen by antigen-presenting cells to the draining lymph nodes, where the antigen is presented to the adaptive immune system.

Truncated Saponin Lacking the Branched Trisaccharide Domain (**16**)

Having established saponin variant **6** (SQS-0-0-5-18) as a potent adjuvant with low toxicity, we next investigated the role of the branched trisaccharide domain in adjuvant activity. We synthesized truncated saponin **16** (SQS-1-0-5-18), which lacks this entire domain, from quillaic acid (**10**)²² and protected trisaccharide **12** (Figure 3a). Remarkably, truncated saponin **16** elicited KLH and MUC1 antibody responses comparable to those of parent aryl iodide **6**, NQS-21, and SQS-21, and significantly higher than those of the no-adjuvant control, with the exception of anti-MUC1 titers at the lower dose (20 µg) (Figures 3b,c). Antibody titers against OVA were also similar to those elicited by parent aryl iodide saponin **6** and considerably higher than those of the no-adjuvant control (Figure 3d). Moreover, truncated saponin **16** exhibited much lower toxicity than NQS-21 and SQS-21, slightly lower than that of even the parent aryl iodide **6** (Figure 3e). Thus, the entire branched trisaccharide domain is not required for adjuvant activity in the truncated saponin variant **16**.

This represents a major simplification of the saponin structure and provides a more favorable activity/toxicity profile than QS-21 itself.

Saponins with Targeted Triterpene Domain Modifications (18–22)

The discovery that the entire branched trisaccharide domain is not required for adjuvant activity facilitated investigation of the triterpene domain of QS-21 by semisynthesis of new variants from alternative triterpene precursors, by analogy to the synthesis of **16** (SQS-1-0-5-18) from quillaic acid (Figure 3a). We were particularly interested in exploring the roles of the C4-aldehyde substituent and C16-alcohol in the quillaic acid core structure. Previously, the C4-aldehyde substituent has been proposed to be important for the adjuvant activity of QS-21¹⁸. However, other saponins that lack a triterpene aldehyde substituent but are active adjuvants have been identified recently^{23,24,25}. Thus, an initial variant **18** (SQS-1-7-5-18) was synthesized from oleanolic acid (Supplementary Fig. 6), which shares the same carbon skeleton as quillaic acid, differing only in the oxidation states at the C4 substituent (Me vs. CHO) and C16 (H vs. OH).

Oleanolic acid derivative **18** (C4-Me, C16-H) led to lower antibody titers against all three antigens compared to the parent quillaic acid derivative **16** (Figure 4a–d). Further, OVA antibody titers with oleanolic acid derivative **18** were similar to those in the no-adjuvant control. Thus, removal of both the C4-aldehyde substituent and C16-alcohol in oleanolic acid derivative **18** results in considerably attenuated antibody responses in this preclinical vaccination model.

To investigate the importance of each of these functionalities individually, we synthesized triterpene variants **19–22**, in which the oxidation states of the C4-aldehyde substituent and C16-alcohol are varied independently (Figure 5a). Caulophyllogenin variant **19** (SQS-1-11-5-18), in which the C4-aldehyde substituent is reduced to a hydroxymethyl group while the C16-alcohol is retained, was accessed from an advanced intermediate in the synthesis of **16** (SQS-1-0-5-18) (Supplementary Fig. 7). Echinocystic acid variant **20** (SQS-1-8-5-18), in which the C4-aldehyde substituent is replaced by a methyl group while the C16-alcohol is again retained, and hederagenin variant **22** (SQS-1-10-5-18), in which the C4-aldehyde substituent is replaced by a hydroxymethyl group and the C16-alcohol is replaced by a proton, were prepared from the corresponding, commercially available triterpenes (Supplementary Fig. 8 and Supplementary Fig. 9). Gypsogenin variant **21** (SQS-1-9-5-18), which possesses the C4-aldehyde substituent but lacks the C16-alcohol, was accessed via initial TEMPO oxidation of the C4-hydroxymethyl substituent in hederagenin to afford gypsogenin (Supplementary Figs. 8 and 9).

These saponin variants were evaluated with a four-component vaccine that comprised MUC1-KLH, OVA, and the poorly immunogenic glycolipid GD3 (melanoma, neuroblastoma, sarcoma antigen) conjugated to KLH (GD3-KLH) (Figure 5b–e; see Supplementary Fig. 10 for full data with both 20 and 50 µg doses). Echinocystic acid derivative **20** (C4-Me, C16-OH), induced the highest antibody responses to all four antigens, comparable to or higher than those of the complete, branched trisaccharide-containing saponin **6** (SQS-0-0-5-18) and QS-21. Caulophyllogenin derivative **19** (C4-CH₂OH, C16-

OH) afforded antibody titers slightly below those of echinocystic acid derivative **20**, branched trisaccharide-containing saponin **6**, and SQS-21, albeit only at elevated doses (50 μg). In contrast, gypsogenin derivative **21** (C4-CHO, C16-H) and hederagenin derivative **22** (C4-CH₂OH, C16-H), both generated lower antibody responses in all cases except the anti-GD3 IgG response, and similar to the no-adjuvant treated controls for KLH and OVA.

Antibody subtyping of the anti-MUC1 and anti-OVA IgG isotypes revealed a significant bias toward the mouse IgG1 and IgG2b subclasses with both of the adjuvant active saponins in this group (**19**, **20**). Similar results were obtained with SQS-21 and with the parent quillaic acid derivative **16**. Production of other mouse IgG subclasses, including IgG2a and IgG3, was low or negligible, as indicated by class-specific ELISA. Toxicity remained drastically lower for all four variants compared to NQS-21 and SQS-21 (Figure 5f).

Thus, echinocystic acid derivative **20** provides immunostimulatory activity generally rivaling that of SQS-21 but without the associated toxicity. Caulophyllogenin derivative **19** also provides antibody responses similar to the complete, branched trisaccharide-containing saponin **6**, although higher doses are required. Importantly, both echinocystic acid derivative **20** and caulophyllogenin derivative **19** lack the C4-aldehyde substituent but retain the C16-alcohol. In contrast, gypsogenin derivative **21** and hederagenin derivative **22** both lack the C16-alcohol and induced lower antibody responses to all antigens tested. Taken together, these data indicate that the C4-aldehyde substituent is not required for potent immunoadjuvant activity in these novel saponins and reveal a previously unappreciated role for the C16-alcohol in enhancing activity.

Biodistribution of Truncated Saponins [¹³¹I]-**16** and [¹³¹I]-**18**

We next compared the *in vivo* biodistribution patterns of the adjuvant-active truncated quillaic acid variant **16** (SQS-1-0-5-18) and the adjuvant-attenuated oleanolic acid derivative **18** (SQS-1-7-5-18), using the radioiodinated congeners [¹³¹I]-**16** (Figure 3a) and [¹³¹I]-**18** (Supplementary Fig. 6), to enable correlation with our earlier studies of the active/attenuated adjuvant pair **6** (SQS-0-0-5-18) and **8** (SQS-0-3-7-18) (Figure 2a). The active adjuvant [¹³¹I]-**16** showed significantly higher localization at the injection site (136% ID/g) and within the lymph nodes (3.55% ID/g) compared to [¹³¹I]-**18** (11.5% and 0.50% ID/g, respectively) (Figure 6). Accordingly, in both biodistribution studies, the more active adjuvant was preferentially retained at the site of injection and accumulated in the lymph nodes, providing a positive correlation between this biodistribution pattern and adjuvant activity.

Discussion

The molecular mechanisms of the adjuvant activity of QS-21 and its variants remain poorly understood. It has been reported that QS-21 stimulates mixed Th1/Th2 helper T cell responses, corresponding to cellular and humoral immunity respectively, including antigen-specific CD8⁺ cytotoxic T lymphocytes.²⁶ There is some evidence to suggest that QS-21 does not bind to Toll-like receptors 2 and 4²⁶ and that it does not operate by a depot effect, in which the adjuvant increases the lifetime of the antigen, extending its presentation to the immune system²⁷. It has also been suggested that *Quillaja* saponins may, by analogy to

tucaresol, bind covalently to amino groups on T cell surface receptors via imine formation at the C4-aldehyde substituent, providing costimulation for T cell activation²⁸.

Herein, extensive structure–function studies of novel iodinated saponins based on QS-21 have identified echinocystic acid derivative **20** (SQS-1-8-5-18) as a minimal saponin immunoadjuvant with potent activity and dramatically reduced toxicity compared to the natural product (Figure 5), as well as improved synthetic accessibility relative to previously reported variants^{16,17}. Subtyping of the IgG antibodies elicited by echinocystic acid derivative **20**, as well as the closely-related quillaic acid derivative **16** (SQS-1-0-5-18) and caulophyllogenin derivative **19** (SQS-1-11-5-18), indicates that IgG1 and IgG2b subclasses predominate. The mouse IgG1 subclass is associated with Th2 cell responses (humoral immunity), whereas the IgG2b, together with the IgG2a, are related to Th1 responses (cellular immunity) and are known to induce potent immunotherapeutic effector functions²⁹, including complement-dependent cytotoxicity and antibody-dependent cellular toxicity. Similar results were obtained with SQS-21. Thus, despite the considerable structural differences between these truncated saponins and QS-21, they elicit both Th1 and Th2 immunity, a hallmark of QS-21 itself.

To date, investigation of structural requirements within the triterpene domain of QS-21 has been hampered by the challenges associated with chemoselective modification of the natural product and by material throughput limitations for synthetic analogues that incorporate alternative triterpenes. Thus, our striking discovery that the entire branched trisaccharide domain can be omitted while retaining potent adjuvant activity and attenuating toxicity has opened the door to investigation of such triterpene modifications by semisynthesis from alternative, readily available triterpene precursors.

These studies revealed that the C4-aldehyde substituent is dispensable for potent adjuvant activity while the C16-hydroxyl group enhances activity in these truncated saponins. In contrast, the C4-aldehyde substituent of QS-21 has been suggested previously to react with amino groups on T-cell surface receptors through Schiff base formation, providing co-stimulation necessary for T-cell activation and Th1 cellular immunity^{18,28}. This hypothesis was based on the finding that reductive amination of the C4-aldehyde substituent of QS-21 provides amine derivatives with significantly attenuated adjuvant activity¹⁸. However, this modification not only removes the C4-aldehyde substituent but also introduces a positively-charged amino group at this position, which may alternatively compromise non-covalent interactions with a putative receptor or otherwise interfere with proper biodistribution or subcellular localization of the adjuvant. Along similar lines, we have previously shown that QS-21 variant **2** (SQS-0-0-5-11), which retains the C4-aldehyde substituent but carries a positively-charged amino functionality in the acyl chain domain, is likewise inactive¹⁷. While it remains possible that QS-21 and these modified, synthetic variants may have distinct molecular targets, they appear to induce similar cellular effects *in vivo*.

Conversely, our finding herein that the C16-hydroxyl group enhances adjuvant activity in these truncated saponins suggests a previously unappreciated role for this functionality, perhaps in stabilizing saponin conformation and/or interacting directly with a putative

receptor. These results are consistent with reports of other adjuvant-active saponins that possess the C16-hydroxyl group but lack the triterpene C4-aldehyde substituent^{23,24,25}.

The development of these iodinated saponins has also enabled comparative *in vivo* biodistribution studies using adjuvant-active/attenuated pairs. We observed a strong positive correlation between adjuvant activity and retention at the site of injection and accumulation in the draining lymph nodes, a known site for immune cell maturation. Fluorescence imaging studies confirmed localization of both the adjuvant and antigen to the nearest draining lymph node only with active adjuvant. While the underlying molecular basis for these observed biodistribution patterns remains to be elucidated, the availability of the adjuvant-active/attenuated pairs discovered herein should facilitate its investigation and further studies of the resulting implications for cellular mechanisms of action.

A review article citing unpublished data has reported that naturally-derived QS-21, injected intramuscularly into rabbits, is absorbed rapidly from the injection site, but similarly accumulates in the draining lymph nodes at 48 h³⁰. Other adjuvants comprised of *Quillaja* saponin mixtures have also been reported to increase cell counts in the lymph nodes³¹ and to increase uptake of Alexa 488-labeled OVA by dendritic cells²⁰. A recent study similarly showed that the adjuvant MF59, an oil-in-water emulsion containing squalene, recruits antigen-presenting cells and other cell types to the draining lymph nodes, and that fluorescent forms of both the adjuvant and OVA antigen are taken up by these cells³². Earlier studies also demonstrated that MF59 localizes to the lymph nodes³³ and is taken up by dendritic cells and colocalizes intracellularly with the antigen gD³⁴. Taken together, these results suggest that *Quillaja* saponins may facilitate antigen trafficking by antigen-presenting cells from the site of injection to the lymph nodes, where the processed antigens are presented to the adaptive immune system. This mechanism, shared by MF59, would contribute to the resulting activation of T-helper cells and generation of high-affinity antibodies from B cells.

In conclusion, we have developed a series of truncated QS-21 variants that exhibit potent adjuvant activity and low toxicity, are synthetically accessible, and have enabled the first *in vivo* mechanistic studies of these structurally-defined, synthetic saponins. Previous, conservative modifications in the acyl chain domain of QS-21 have successfully decoupled adjuvant activity from toxicity¹⁶. Synthetically more-tractable variants have also been developed, albeit without reduction in toxicity¹⁷. The novel saponins described herein achieve both goals, with echinocystic acid derivative **20** (SQS-1-8-5-18) representing a particularly compelling candidate for further advancement toward clinical evaluation. While these saponins appear to induce biological effects similar to those of MF59, the remarkable potency of QS-21 and these novel variants compared to many other adjuvants tested previously^{5,35} suggests that they may have additional activities beyond the biodistribution effects demonstrated herein. The development of this minimal saponin adjuvant platform sets the stage for further investigations of the molecular mechanisms of saponin immunostimulation using, for example, photoaffinity probe variants for target identification. It will also be of interest to assess cytokine production, T-cell responses, and the cytotoxicity of antibodies elicited in vaccinations using these novel immunoadjuvants. Convenient synthetic access to this small library of improved, adjuvant-active saponins may

also allow screening with other antigens of interest to define optimal adjuvant–antigen pairs in the future.

Material and Methods

General synthetic methods

Reactions were performed in flame-dried sealed-tubes or modified Schlenk (Kjeldahl shape) flasks fitted with a glass stopper under a positive pressure of argon, unless otherwise noted. Air- and moisture-sensitive liquids and solutions were transferred via syringe. The appropriate carbohydrate reagents were dried via azeotropic removal of water with toluene. Molecular sieves were activated at 350 °C and were crushed immediately prior to use, then flame-dried under vacuum. Organic solutions were concentrated by rotary evaporation below 30 °C. Flash column chromatography was performed employing 230–400 mesh silica gel. Thin-layer chromatography was performed using glass plates pre-coated to a depth of 0.25 mm with 230–400 mesh silica gel impregnated with a fluorescent indicator (254 nm). Additional protocols, detailed experimental procedures, and complete analytical data for all isolable synthetic intermediates are in Supplementary Methods.

General procedure for synthesis of truncated saponins

The requisite triterpene cores were selectively silylated (TESOTf, 2,6-lutidine) at hydroxyl groups to provide protected triterpenes having a free C28-carboxylic acid. β -Selective Schmidt glycosylation ($\text{BF}_3\cdot\text{OEt}_2$) with trisaccharide trichloroacetimidate donor **12** (ref. 17) followed by reduction of the azide (PhSeH) gave the corresponding glycosyl esters. Acylation of the amine with 6-((*t*-butoxycarbonyl)-amino)hexanoic acid (**14**) (EtOCOCCl , Et_3N) and subsequent global deprotection by hydrogenolysis (H_2 , Pd/C) and acid hydrolysis ($\text{TFA}/\text{H}_2\text{O}$) afforded the fully deprotected saponins bearing the free amine at the terminus of the acyl chain domain. Late-stage acylation of the amine with succinimidyl esters **4** or **5** gave the corresponding aryl iodides **16**, **18–22** or the relevant aryl tin congeners, respectively. See Figure 3a, Supplementary Figs. 6–9 and Supplementary Methods for complete details.

General procedure for preclinical mouse vaccination model

Groups of five mice (C57BL/6J, female, 6–8 weeks of age) were vaccinated with a three-component vaccine consisting of MUC1-KLH (2.5 μg) and OVA (20 μg), or a four-component vaccine that also included GD3-KLH (5 μg). Antigens were co-administered with the adjuvant of interest (5, 20, or 50 μg) or without adjuvant (no-adjuvant control) in phosphate buffered saline (PBS, 100 μL) via subcutaneous injections on days 0, 7, and 14, followed by a booster on day 65. Mouse sera were collected at day 72 and antibody titers against each antigen were determined by ELISA. Statistical significance of each antibody response compared to the no-adjuvant control was assessed using a two-tailed unpaired Student's *t*-test with CI = 95%. As an initial, general assessment of toxicity, mouse weight loss was monitored on days 0, 1, 2, 3, and 7 after the first vaccination. These animal experiments were conducted as described in MSKCC Institutional Animal Care and Use Committee (IACUC) protocol #97-11-051. See Supplementary Methods for complete details.

Radiosynthesis

The aryl tin saponins (**7**, **9**, **17**, **S9**) were synthesized from the corresponding amine precursors (**2**, **S4**, **15**, **S8**) by acylation with *N*-succinimidyl-4-(trimethylstannyl)benzoate **5** (Et₃N, DMF, 21 °C, 1-2.5 h). Radiolabeling was achieved by iodination of the aryl tin saponin (20 µg) with [¹³¹I]-NaI and chloramine-T (methanol, 21 °C, 1 min), followed by immediate HPLC purification. Solvents were removed by rotary evaporation at 35 °C and the radioiodinated probes were formulated in 0.9% saline for biodistribution studies. Co-elution of the radioiodinated probes with the corresponding cold saponins was used for quality control analysis.

Radiolabeled ovalbumin was synthesized by treating 20 µg of ovalbumin with [¹³¹I]-NaI and Chloramine-T in methanol. The reaction mixture was diluted with 2 mL phosphate buffered saline (PBS) followed by centrifugal filtration at 2800 rpm (736 g) for 12 min using a 30 kDa molecular weight cutoff filter. This process was repeated twice and the concentrated compound was then formulated in 1 mL 0.9% saline for biodistribution studies.

Biodistribution experiments

Groups of five mice (naive, C57BL/6J female, 8–10 weeks of age) were injected subcutaneously with the radioiodinated saponin variants of interest (~25 µCi), the corresponding non-radiolabeled saponin (20 µg), and OVA (20 µg) in PBS (150 µL). Mice were sacrificed at 24 h, 72 h, and 96 h post-injection. Tissues and organs were harvested and analyzed for distribution of radioactivity normalized to the weight of the organ (%ID/g, percent injected dose per gram). Statistical significance of the difference in recoveries (%ID/g) for the active and attenuated adjuvant was assessed for each tissue or organ using two-tailed unpaired Student's *t*-test with CI = 95%. In initial experiments, biodistribution profiles did not change substantially between 24 h and 96 h post-injection (Supplementary Fig. 2), and the 24 h time-point was used for the subsequent experiments. These animal experiments were conducted as described in MSKCC IACUC protocol #08-07-013.

Imaging studies

Three mice were shaved and immunized in the left flank with 10 µg of active adjuvant **3** (SQS-0-0-5-12) or inactive adjuvant **2** (SQS-0-0-5-11) and 20 µg of Alexa-647-conjugated OVA (OVA-A647) in PBS (100 µL). Whole-body imaging was performed at 24 h post-injection with a Maestro Imaging System. At 24 h post-injection, mice were sacrificed and the left and right lymph nodes were dissected and imaged separately. These animal experiments were conducted as described in MSKCC IACUC protocol #97-11-051.

Supplementary Material

Refer to Web version on PubMed Central for supplementary material.

Acknowledgments

Dedicated to the memory of our mentor and colleague, David Y. Gin (1967–2011). We thank S. J. Danishefsky, M. M. Adams, and W. E. Walkowicz for helpful discussions, G. Sukenick, H. Liu, H. Fang, and S. Rusli for expert NMR and mass spectral support and K. K. Sevak, N. Ramos, and C. B. Davis for technical support with biodistribution and radiometric studies. Generous financial support was provided by the European Commission

(Marie Curie International Outgoing Fellowship to A.F.-T.), the NIH (R01 AI085622 to J.S.L. and D.Y.G. and R01 GM058833 to D.S.T. and D.Y.G.), William and Alice Goodwin and the Commonwealth Foundation for Cancer Research, and the Experimental Therapeutics Center of MSKCC.

References

1. Moyle PM, Toth I. Modern subunit vaccines: development, components, and research opportunities. *ChemMedChem*. 2013; 8:360–376. [PubMed: 23316023]
2. Leroux-Roels G. Unmet needs in modern vaccinology: adjuvants to improve the immune response. *Vaccine*. 2010; 28:C25–C36. [PubMed: 20713254]
3. Reed SG, et al. New horizons in adjuvants for vaccine development. *Trends Immunol*. 2009; 30:23–32. [PubMed: 19059004]
4. Kensil CR, Patel U, Lennick M, Marciani D. Separation and characterization of saponins with adjuvant activity from *Quillaja saponaria* Molina cortex. *J Immunol*. 1991; 146:431–437. [PubMed: 1987271]
5. Kim SK, et al. Comparison of the effect of different immunological adjuvants on the antibody and T-cell response to immunization with MUC1-KLH and GD3-KLH conjugate cancer vaccines. *Vaccine*. 1999; 18:597–603. [PubMed: 10547417]
6. Soltysik S, Bedore DA, Kensil CR. Adjuvant activity of QS-21 isomers. *Ann N Y Acad Sci*. 1993; 690:392–395. [PubMed: 8368766]
7. Jacobsen NE, et al. Structure of the saponin adjuvant QS-21 and its base-catalyzed isomerization product by ^1H and natural abundance ^{13}C NMR spectroscopy. *Carbohydr Res*. 1996; 280:1–14. [PubMed: 8581890]
8. Ragupathi G, Gardner JR, Livingston PO, Gin DY. Natural and synthetic saponin adjuvant QS-21 for vaccines against cancer. *Expert Rev Vaccines*. 2011; 10:463–470. [PubMed: 21506644]
9. Agnandji ST, et al. First results of Phase 3 trial of RTS,S/AS01 malaria vaccine in African children. *New Engl J Med*. 2011; 365:1863–1875. [PubMed: 22007715]
10. Kennedy JS, et al. The safety and tolerability of an HIV-1 DNA prime-protein boost vaccine (DP6-001) in healthy adult volunteers. *Vaccine*. 2008; 26:4420–4424. [PubMed: 18588934]
11. Vandepapeliere P, et al. Vaccine Adjuvant Systems containing monophosphoryl lipid A and QS21 induce strong and persistent humoral and T cell responses against hepatitis B surface antigen in healthy adult volunteers. *Vaccine*. 2008; 26:1375–1386. [PubMed: 18272264]
12. Von Eschen K, et al. The candidate tuberculosis vaccine Mtb72F/AS02A: Tolerability and immunogenicity in humans. *Hum Vaccin*. 2009; 5:475–482. [PubMed: 19587528]
13. Vellas B, et al. Long-term follow-up of patients immunized with AN1792: reduced functional decline in antibody responders. *Curr Alzheimer Res*. 2009; 6:144–151. [PubMed: 19355849]
14. Wang P, Kim YJ, Navarro-Villalobos M, Rohde BD, Gin DY. Synthesis of the potent immunostimulatory adjuvant QS-21A. *J Am Chem Soc*. 2005; 127:3256–3257. [PubMed: 15755124]
15. Deng K, et al. Synthesis of QS-21-xylose: establishment of the immunopotentiating activity of synthetic QS-21 adjuvant with a melanoma vaccine. *Angew Chem, Int Ed*. 2008; 47:6395–6398.
16. Adams MM, et al. Design and synthesis of potent *Quillaja* saponin vaccine adjuvants. *J Am Chem Soc*. 2010; 132:1939–1945. [PubMed: 20088518]
17. Chea EK, et al. Synthesis and preclinical evaluation of QS-21 variants leading to simplified vaccine adjuvants and mechanistic probes. *J Am Chem Soc*. 2012; 134:13448–13457. [PubMed: 22866694]
18. Soltysik S, et al. Structure/function studies of QS-21 adjuvant: assessment of triterpene aldehyde and glucuronic acid roles in adjuvant function. *Vaccine*. 1995; 13:1403–1410. [PubMed: 8578817]
19. Seevers RH, Counsell RE. Radioiodination techniques for small organic molecules. *Chem Rev*. 1982; 82:575–590.
20. Duewell P, et al. ISCOMATRIX adjuvant combines immune activation with antigen delivery to dendritic cells *in vivo* leading to effective cross-priming of CD8⁺ T cells. *J Immunol*. 2011; 187:55–63. [PubMed: 21613613]

21. Scott MT, Goss-Sampson M, Bomford R. Adjuvant activity of saponin: antigen localization studies. *Int Arch Allergy Appl Immunol.* 1985; 77:409–412. [PubMed: 4018882]
22. Elliott DF, Kon GAR. Sapogenins. VI. Quillaic acid. *J Chem Soc.* 1939:1130–1135.
23. Nico D, Santos FN, Borja-Cabrera GP, Palatnik M, Palatnik de Sousa CB. Assessment of the monoterpene, glycidic and triterpene-moieties' contributions to the adjuvant function of the CP05 saponin of *Calliandra pulcherrima* Benth during vaccination against experimental visceral leishmaniasis. *Vaccine.* 2007; 25:649–658. [PubMed: 17014936]
24. Castro-Diaz N, et al. Saponins from the Spanish saffron *Crocus sativus* are efficient adjuvants for protein-based vaccines. *Vaccine.* 2012; 30:388–397. [PubMed: 22079266]
25. Oda K, et al. Adjuvant and haemolytic activities of 47 saponins derived from medicinal and food plants. *Biol Chem.* 2000; 381:67–74. [PubMed: 10722052]
26. Pink JR, Kieny MP. 4th Meeting on novel adjuvants currently in/close to human clinical testing. *Vaccine.* 2004; 22:2097–2102. [PubMed: 15212010]
27. Kensil CR. Saponins as vaccine adjuvants. *Crit Rev Ther Drug Carrier Syst.* 1996; 13:1–55. [PubMed: 8853958]
28. Marciani DJ. Vaccine adjuvants: role and mechanisms of action in vaccine immunogenicity. *Drug Discov Today.* 2003; 8:934–943. [PubMed: 14554157]
29. Nimmerjahn F, Ravetch JV. Divergent immunoglobulin G subclass activity through selective Fc receptor binding. *Science.* 2005; 310:1510–1512. [PubMed: 16322460]
30. Kensil CR, Kammer R. QS-21: a water-soluble triterpene glycoside adjuvant. *Exp Opin Invest Drugs.* 1998; 7:1475–1482.
31. Bomford R. Studies on the cellular site of action of the adjuvant activity of saponin for sheep erythrocytes. *Int Arch Allergy Appl Immunol.* 1982; 67:127–131. [PubMed: 7035375]
32. Calabro S, et al. Vaccine adjuvants alum and MF59 induce rapid recruitment of neutrophils and monocytes that participate in antigen transport to draining lymph nodes. *Vaccine.* 2011; 29:1812–1823. [PubMed: 21215831]
33. Dupuis M, McDonald DM, Ott G. Distribution of adjuvant MF59 and antigen gD2 after intramuscular injection in mice. *Vaccine.* 1999; 18:434–439. [PubMed: 10519932]
34. Dupuis M, et al. Dendritic cells internalize vaccine adjuvant after intramuscular injection. *Cell Immunol.* 1998; 186:18–27. [PubMed: 9637761]
35. Kim SK, Ragupathi G, Cappello S, Kagan E, Livingston PO. Effect of immunological adjuvant combinations on the antibody and T-cell response to vaccination with MUC1-KLH and GD3-KLH conjugates. *Vaccine.* 2000; 19:530–537. [PubMed: 11027818]

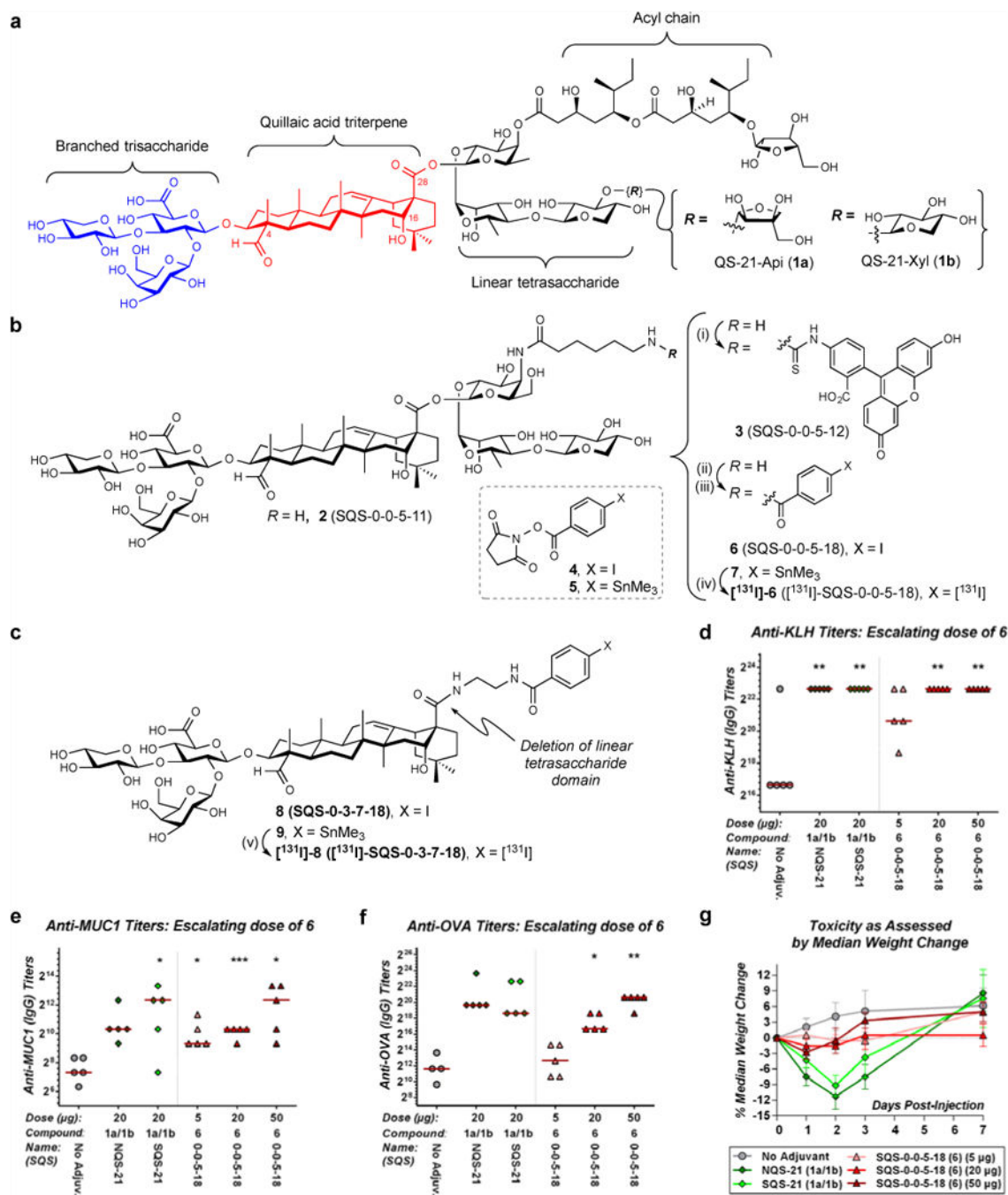


Figure 1. Aryl iodide saponin 6 exhibits potent adjuvant activity and low toxicity in a preclinical mouse vaccination model

(a) Structure of QS-21 and its four key structural domains. (b) Synthesis of aryl iodide saponins **6** (SQS-0-0-5-18) and [¹³¹I]-**6**: (i) FITC, Et₃N, DMF, 21 °C, 2 h, 75%; (ii) **4**, Et₃N, DMF, 21 °C, 1 h, 52%; (iii) **5**, Et₃N, DMF, 21 °C, 1 h, 75%; (iv) [¹³¹I]-NaI, Chloramine-T, MeOH, 21 °C, 1 min, >50%. (c) Structure of adjuvant-attenuated negative control saponin **8** (SQS-0-3-7-18) and synthesis of [¹³¹I]-**8**: (v) [¹³¹I]-NaI, Chloramine-T, MeOH, 21 °C, 1 min, >50%. Biological evaluation of aryl iodide saponin **6** (SQS-0-0-5-18) with three-

component vaccine for **(d)** anti-KLH titers (IgG), **(e)** anti-MUC1 titers (IgG), and **(f)** anti-OVA titers (IgG) indicating potent adjuvant activity comparable to natural and synthetic QS-21 (compare 20 μ g doses); horizontal bars indicate median titers; statistical significance compared to no-adjuvant control: * = $p < 0.05$, ** = $p < 0.01$, *** = $p < 0.001$. **(g)** Toxicity assessment based on median percent weight loss, indicating low toxicity of **6** (SQS-0-0-5-18); error bars indicate maximum and minimum values for five mice.

Author Manuscript

Author Manuscript

Author Manuscript

Author Manuscript

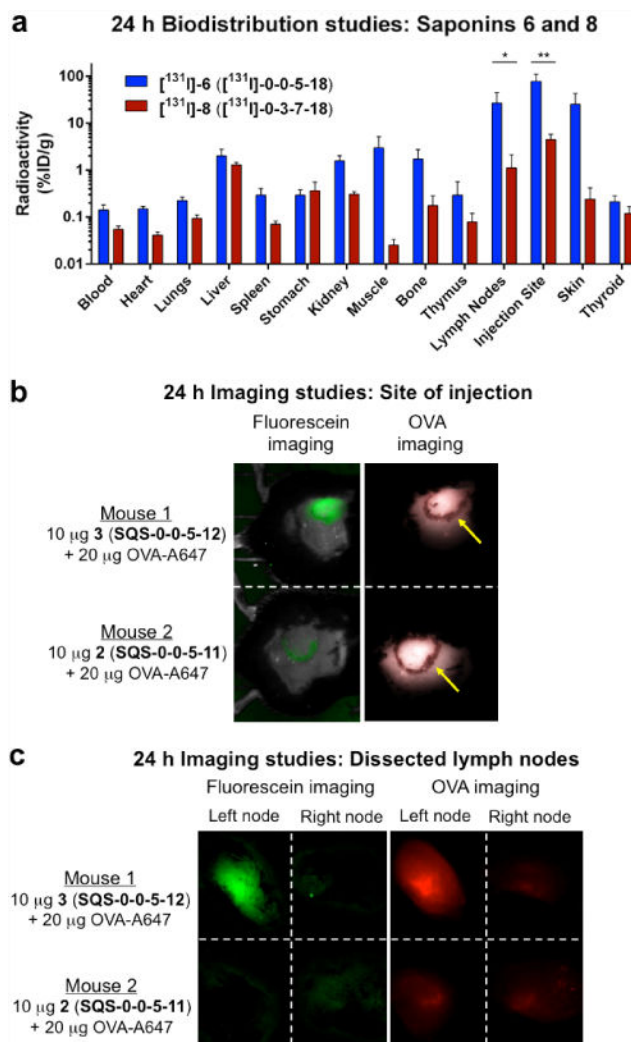


Figure 2. Radioiodinated saponin $[^{131}\text{I}]$ -6 and fluorescent saponin 3 localize to lymph nodes and injection site in mice

(a) Biodistribution of active adjuvant $[^{131}\text{I}]$ -6 ($[^{131}\text{I}]$ -SQS-0-0-5-18) and attenuated adjuvant $[^{131}\text{I}]$ -8 ($[^{131}\text{I}]$ -SQS-0-3-7-18) with OVA antigen, indicating accumulation of $[^{131}\text{I}]$ -6, but not $[^{131}\text{I}]$ -8, at injection site and lymph nodes (see Supplementary Fig. 2); error bars indicate standard deviation from mean for five mice; statistical significance indicated graphically only for lymph nodes and injection site for clarity: * = $p < 0.05$: liver, muscle, lymph node, skin, thyroid; ** = $p < 0.01$: blood, lungs, spleen, kidneys, bone, injection site; *** = $p < 0.001$: heart. (b) Imaging at injection site (yellow arrows indicate ink circles) with fluorescein-labeled active adjuvant **3** (SQS-0-0-5-12) or unlabeled inactive adjuvant **2** (SQS-0-0-5-11) and Alexa-647-labeled OVA (OVA-A647), indicating retention of **3** and OVA-A647 at injection site; green crescent in fluorescein image for Mouse 2 is due to software ghosting effect (see Supplementary Fig. 5). (c) Imaging of dissected lymph nodes with active adjuvant **3** (SQS-0-0-5-12) or inactive adjuvant **2** (SQS-0-0-5-11) and OVA-A647, indicating increased accumulation of OVA-A647 with **3** but not **2**. Mice were injected in left flank and right lymph node serves as negative control within each animal.

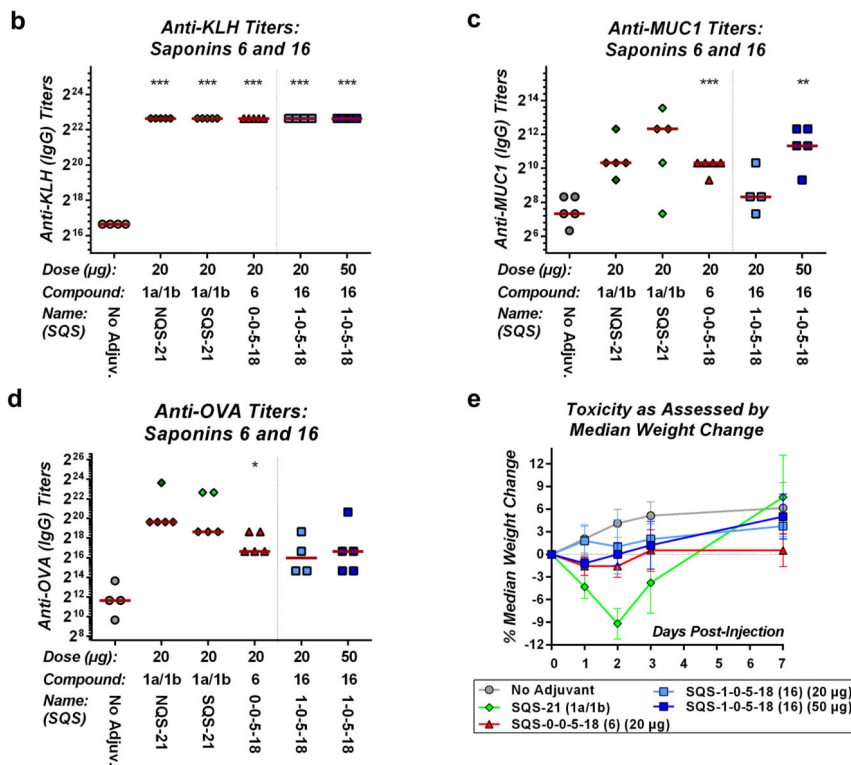
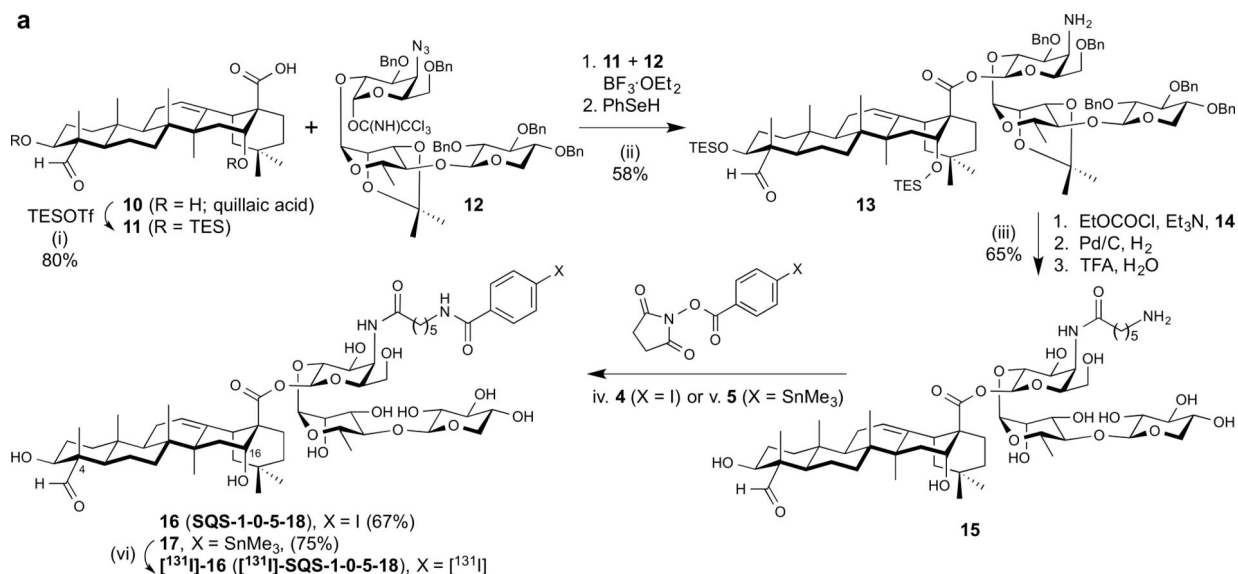


Figure 3. Truncated saponin 16 lacks the entire branched trisaccharide domain of QS-21 but retains potent adjuvant activity and low toxicity in a preclinical mouse vaccination model

(a) Synthesis of aryl iodide saponins **16** (SQS-1-0-5-18) and [¹³¹I]-**16**. (i) TESOTf, 2,6-lutidine, CH₂Cl₂, 0 °C, 1 h, 80%; (ii) 1. **11**, **12**, BF₃·OEt₂, 4 Å M.S., CH₂Cl₂, -35 °C, 30 min; 2. PhSeH, Et₃N, 38 °C, 8 h, 58% (2 steps); (iii) 1. HO₂C(CH₂)₅NHBoc (**14**), EtOCOCl, Et₃N, THF, 0 °C, 2.5 h, (acid preactivation), then add to **13**, 0 °C, 1.5 h; 2. H₂ (50 psi), Pd/C (Degussa), THF/EtOH (1:1), 21 °C, 24 h; 3. TFA/H₂O (4:1), 0 °C, 2 h, 65% (3 steps); (iv) **4**, Et₃N, DMF, 21 °C, 2 h, 67%; (v) **5**, Et₃N, DMF, 21 °C, 1.5 h, 75%; (vi)

[¹³¹I]-NaI, Chloramine-T, MeOH, 21 °C, 1 min, 55%. Biological evaluation of truncated saponin **16** with three-component vaccine for **(b)** anti-KLH (IgG), **(c)** anti-MUC1 (IgG) and **(d)** anti-OVA (IgG) titers, indicating potent adjuvant activity; horizontal bars indicate median titers; statistical significance compared to no-adjuvant control: * = $p < 0.05$, ** = $p < 0.01$, *** = $p < 0.001$. **(e)** Toxicity assessment based on median percent weight loss, indicating low toxicity of **16** (SQS-1-0-5-18); error bars indicate maximum and minimum values for five mice.

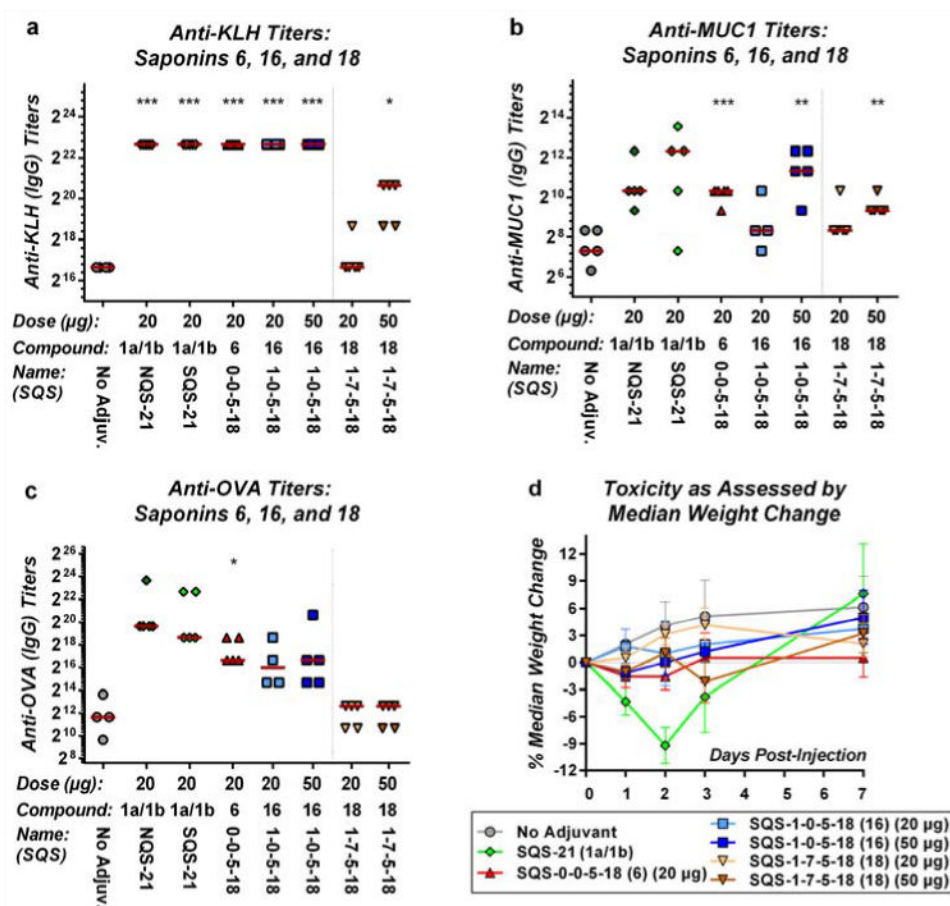


Figure 4. Oleanolic acid derivative **18**, which lacks both the C4-aldehyde substituent and C16-alcohol in the triterpene domain of QS-21, exhibits poor adjuvant activity in a preclinical mouse vaccination model

Biological evaluation of oleanolic acid derivative **18** (SQS-1-7-5-18) with a three-component vaccine for (a) anti-KLH titers (IgG), (b) anti-MUC1 titers (IgG) and (c) anti-OVA titers (IgG), indicating attenuated adjuvant activity; horizontal bars indicate median titers; statistical significance compared to no-adjuvant control: * = $p < 0.05$, ** = $p < 0.01$, *** = $p < 0.001$. (d) Toxicity assessment based on median percent weight, indicating low toxicity of **18** (SQS-1-7-5-18); error bars indicate maximum and minimum values for five mice.

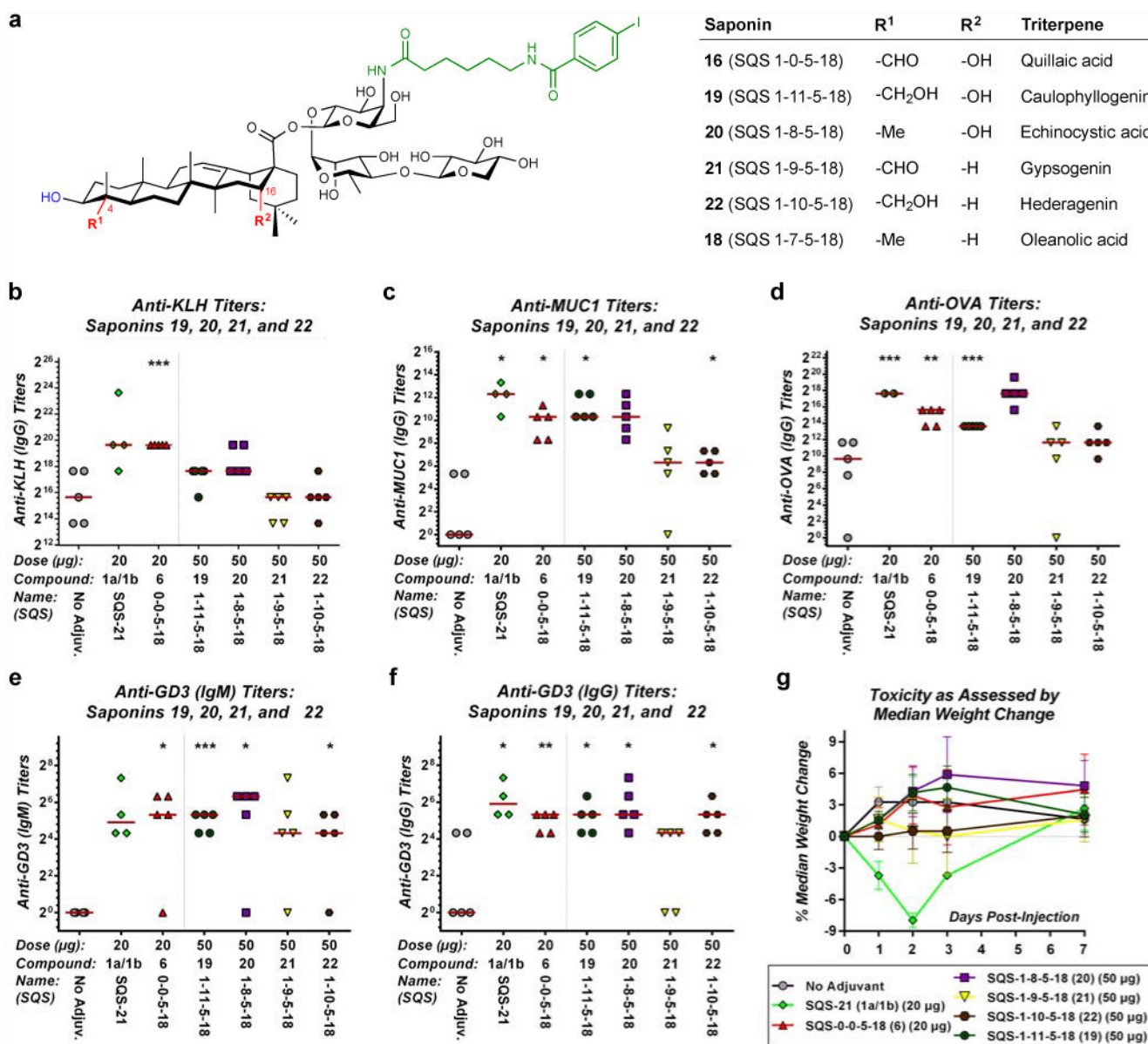


Figure 5. Caulophyllogenin derivative 19 and echinocystic acid derivative 20, which lack the C4-aldehyde substituent but retain the C16-alcohol in the triterpene domain of QS-21, exhibit potent adjuvant activity and no toxicity in a preclinical mouse vaccination model
(a) Structures of saponin variants **19–22** with modifications at the C4-aldehyde substituent and C16-alcohol of the triterpene domain of QS-21. Biological evaluation of triterpene variants **19–22** with a four-component vaccine (MUC1-KLH, OVA, GD3-KLH) for **(b)** anti-KLH (IgG), **(c)** anti-MUC1 (IgG), **(d)** anti-OVA (IgG), **(e)** anti-GD3 (IgM), and **(f)** anti-GD3 (IgG) titers, indicating that the C4-aldehyde substituent is not required adjuvant activity (**19, 20**) while removal of the C16-alcohol attenuates activity (**21, 22**) (see Supplementary Fig. 10 for full data with both 20 and 50 µg doses); horizontal bars indicate median titers; statistical significance compared to no-adjuvant control: * = $p < 0.05$, ** = $p < 0.01$, *** = $p < 0.001$. **(g)** Toxicity assessment based on median percent weight loss,

indicating lack of toxicity of **19–22**; error bars indicate maximum and minimum values for five mice.

Author Manuscript

Author Manuscript

Author Manuscript

Author Manuscript

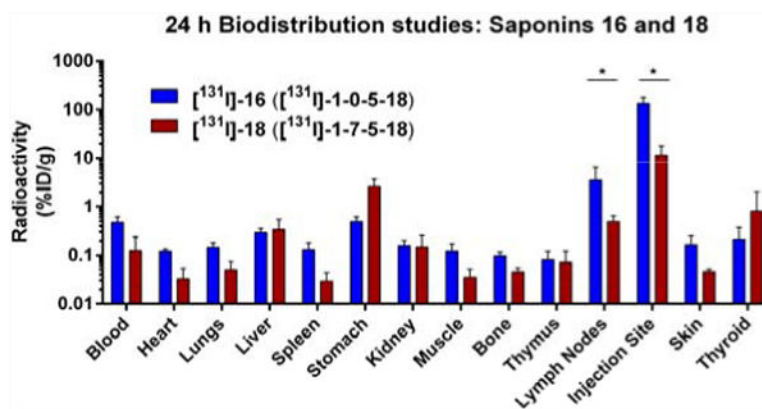


Figure 6. Adjuvant-active quillaic acid derivative 16 localizes to the injection site and lymph nodes in mice while adjuvant-attenuated oleanolic acid derivative 18 does not

In vivo biodistribution in mice of active adjuvant [¹³¹I]-**16** ([¹³¹I]-SQS-1-0-5-18) and attenuated adjuvant [¹³¹I]-**18** ([¹³¹I]-SQS-1-7-5-18) at 24 h post-injection in the presence of 20 μg of OVA; error bars indicate standard deviation from mean for five mice; statistical significance indicated graphically only for lymph nodes and injection site for clarity: * = p 0.05: lymph nodes, injection site, skin; ** = p < 0.01: lungs, spleen, stomach, muscle, bone; *** = p < 0.001: blood, heart.